High fidelity, High order Large Eddy Simulations of Real Geometry Nose Landing Gear on Hybrid Unstructured Grids

Yi Lu[1] and A. A. Demargne[2]
Cambridge Flow Solutions Ltd, Compass House, Vision Park, Histon, Cambridge CB24 9AD, UK

Kai Liu[3]
BoXeR Solutions KK, Chuo-ku, Kobe, Japan, 651-0087

W.N. Dawes[4]
Whittle Lab, University of Cambridge, Cambridge, CB3 0DY, UK

Fast, high fidelity and high order Large Eddy Simulations have been performed for a complex, multi-scale, real geometry nose landing gear configuration on a small scale many-core computing cluster based on the Intel PHI co-processor. This configuration has experimental test data for both aerodynamics and aeroacoustics available from NASA. The generation of a coarse, hybrid unstructured, high geometry fidelity, high order mesh based on a standard, commercially available, low order (piecewise linear) mesher is introduced in this paper. The coarseness is needed to support high order discretized simulations for complex geometries with much fewer degrees of freedoms than lower order methods. Our innovative space time extention of the high order Flux Reconstruction method (STEFR), which allows local time stepping, is efficiently implemented on the many-core computing system and demonstrates the capability to compute unsteady flowfields using LES for industrial class problems on a very modest number of processors and memory size. Comparisons between both time-averaged and instantaneous simulations and experiment data are presented and discussed in this paper.

Nomenclature

BART	Basic Aerodynamic Research Tunnel
CFD	Computational fluid dynamics
DOF	degree of freedoms
LES	large eddy simulation
HPC	high performance computing
PIV	particle image velocimetry
RANS	Reynolds-averaged Navier-Stokes
SPL	sound pressure level
TKE	turbulence kinetic energy, $[(u'^2 + v'^2 + w'^2)/2]$
dt	time step
K	order of polynomials
t	physical time of simulation
T_c	flow passing(through typical length scale) time of LES
UFAFF	University of Florida Aeroacoustic Flow Facility
u, v, w	Cartesian fluid velocity components

[1] CFD Engineer, Cambridge Flow Solutions LTD, Cambridge, UK, and AIAA Associate Member.

[2] Business Development Manager, Cambridge Flow Solutions Ltd, Cambridge, UK, and AIAA Associate Member.

[3] CFD Engineer, BoXeR Solutions KK, Kobe, Japan.

[4] Professor, Whittle Lab, University of Cambridge, UK, and Senior AIAA Member.

X, Y, Z Cartesian coordinates
θ circumferential angle, measured clockwise from wheel leading angle
ρ density

Superscript:
$'$ perturbuton quantity (e.g. $u' = u - u_\infty$)

Subscript:
∞ free-stream quantity

I. Introduction

In recent years, with increasing computing power and the development of numerical algorithms, high fidelity flow simulations for industrial problems become more and more attractive. For instance, airframe noise analysis, for which the landing gear is one of the main contributor during both approach and landing for commercial aircraft.[1] There are several extreme challenges for accurate prediction of noise sources around the landing gear of an aircraft:

1). Geometry complexity: real geometry is necessary for the simulations due to the complexity and sensitivity of the flow field especially for the requirement of noise analysis. Appropriate meshes should be generated to support the solver to resolve boundary layer, shear layer and wake regions.

2). Highly chaotic unsteady flow fields: according to the series of simulations for the same case in this paper by Vasta etc[2] from NASA Langley research center, the better resolution of small scale of turbulence and unsteadiness could achieve better agreement with experiment data.

3). Computational cost: the high fidelity simulations on such a complex, real geometry for the landing gear, need huge computational resource.

In this paper, the flow simulation system, HOTNewt, under development at Cambridge Flow Solution Ltd[3], is described with the aim of performing fast and accurate simulations for cases like landing gear aeroacoustic analysis using very limited computing resource. This paper describes the following solutions for the above challenges:

1). Level set octree based high order coarse mesh generation: the commericial mesh generation software, BOXERMesh[4], which is fully parallized and scales on distributed memory, is highly CAD-tolerant, has scripted integration and automation for high quality mesh generation of large-scale, complex geometries. The functionality for the high order coarse mesh generation and smoothing are extensions to BOXERMesh[5], and are applied to complex simulations in this paper.

2). High order space time extension of the Flux Reconstruction (STEFR) discretisations: the high order flux reconstruction method for 1D problems was originally introduced by Huynh[6] in 2007, extended and implemented to general 3D hybrid meshes including tetrahedrons, prisms, pyramids and hexahedrons[7] in 2012, which could achieve arbitrary high order completely local incell, and very high efficient special discretization with its simple differential form. Later, in 2014, the STEFR method was introduced and validated for varies of simulations[5,8,9], which allows time accurate local time stepping, and could achieve very high speed up ratios for large-scale, multi-scale complex geometries such the real geometry landing gear simulations, compared to conventional uniform time-stepping for unsteady simulations. With the support of high order coarse mesh generation, the required number of degrees of freedom (DOFs) to resolve highly unsteady flowfields are much less than second order finite volume solver by using high order in-cell discretization in both space and time.

3). Partly wall-resolved LES by adopting of an adaptive non-equilibrium wall-model: although higher DOF efficiency and highly reduced FLOPs requirement with time accurate local time stepping, the fully wall-resolved LES is still too expensive for the complex landing gear configurations with high Reynolds number on modest computer resource. Therefore, an adaptive non-equilibrium wall-model is adopted in HOTNewt, to reduce the near wall cell counts in some regions where the turbulence scales don't influence the noise analysis significantly, and the truncation between modeled part and wall-resolved part is smooth by the nature of the adaptivity of the wall-model.

4). Efficient implementation on many core computing systems: in order to achieve higher economic and energy (running) efficiency for the large scale LES simulation, the HOTNewt code is implemented on Intel PHI co-processor in offload mode to make use of the very high computing ability of this modern many-core system, and combined with normal CPUs to produce a heterogeneous computing environment, to enable a very special and optimum balance between computing ability and memory comsuming, details are presented in section IV.

Accordingly, this paper is structured as follows. First, the geometry and simulated configuration are introduced together with the high order coarse mesh generation. Next, the governing equations and the flow solver are reviewed. Then, the implementation of the solver on a low cost, heterogeneous, many-core computing system is presented. Finally, the numerical simulations are presented and discussed snd some conclusions are drawn.

II.   Geometry, Simulated Configuration and mesh generation

The test model is a ¼-scale, high-fidelity replica of a Gulfstream G550 nose landing gear which includes part of the lower fuselage section, as shown in Fig. 1. A series of wind tunnel experiments has been performed[10] in the Basic Aerodynamic Research Tunnel (BART) at NASA Langley Research Center for extensive aerodynamic measurements, and in the open-jet University of Florida Aeroacoustic Flow Facility (UFAFF) mainly for corresponding acoustic measurements. A schematic of the computational domain for current simulations is shown in Fig.2., in which the entire model is suspended in free space for accurate far field acoustic prediction, the top surface of the plate (mounting plate) is set as inviscid while the under surface which accommodating the fuselage and the nose gear are treated as viscous boundary.
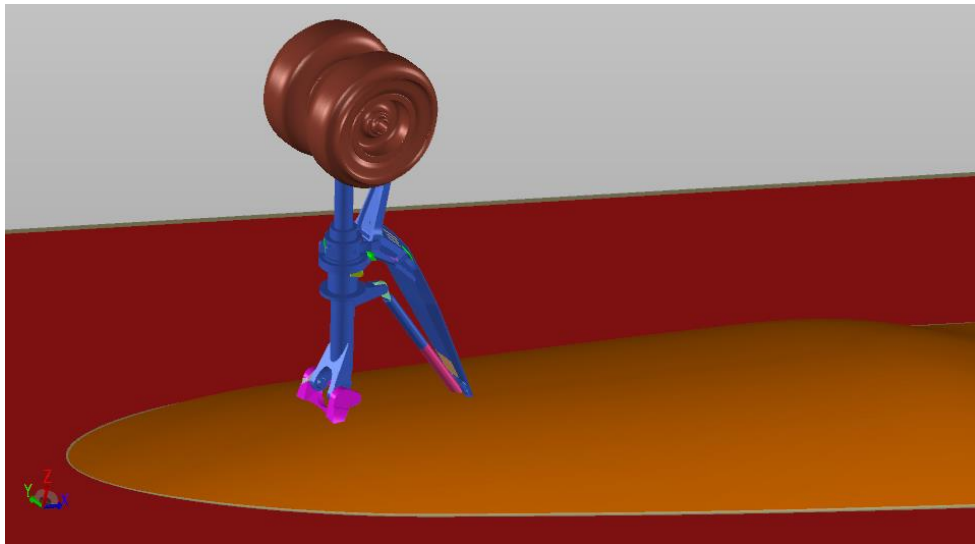

Figure 1. Partially dressed nose landing gear model as tested in BART
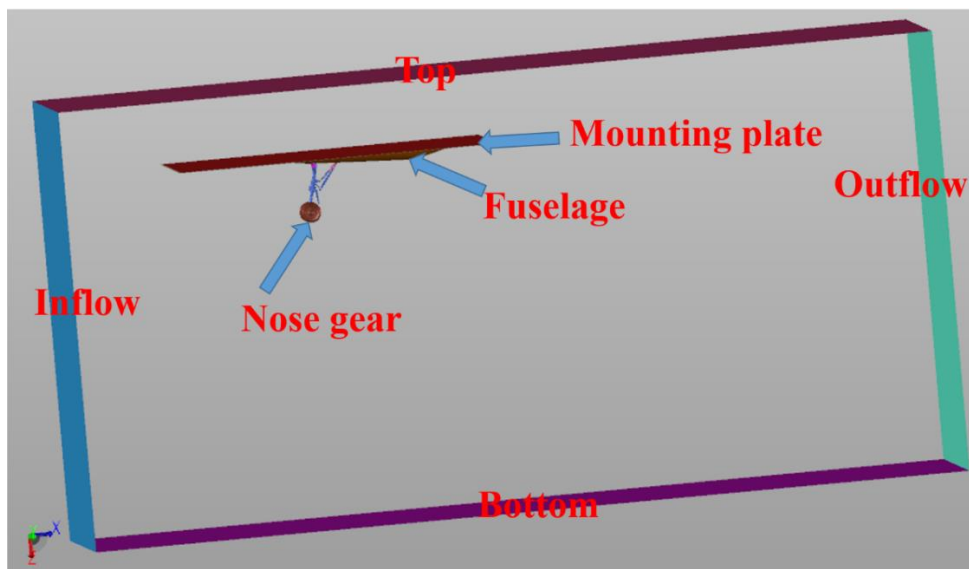

Figure 2. Computational model inside of the domain tailored for better far field acoustic prediction

The current simulations were performed at a freestream Mach number of 0.166, which is identical as the experiments which consist of both aerodynamics and acoustic measurements. The detail farfield flow parameters are set as $u_\infty = 56.3\text{m/s}, T_\infty = 286°\text{C}, P_\infty = 99241\text{Pa}$, which results in a Reynolds number of 7.3×10^4 based on the main strut (piston) diameter.
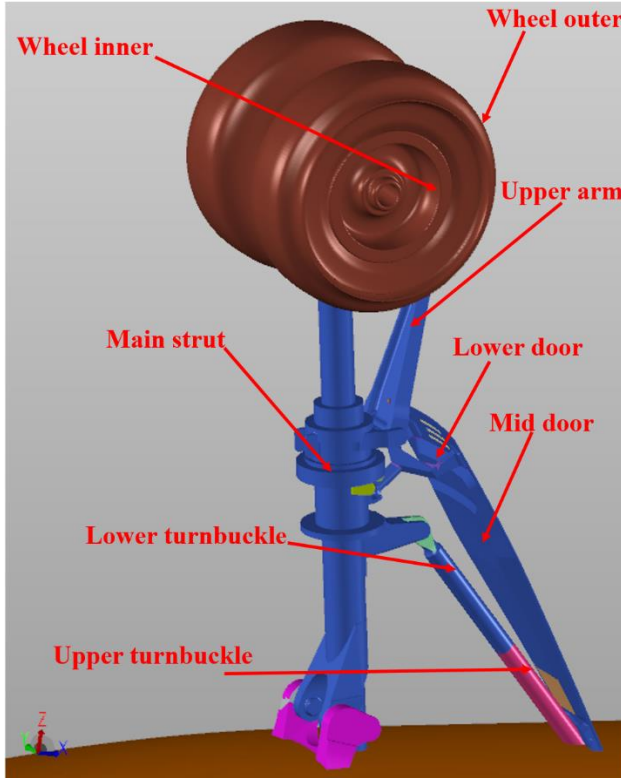

Figure 3. Locations of the unsteady pressure transducers
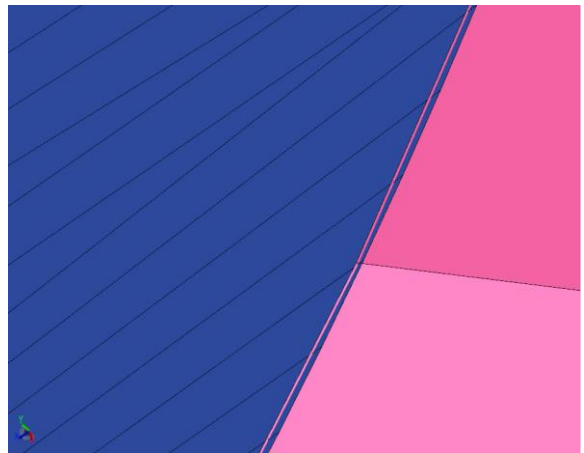
Figure 4. Dirty CAD with a small gap not fully sealed
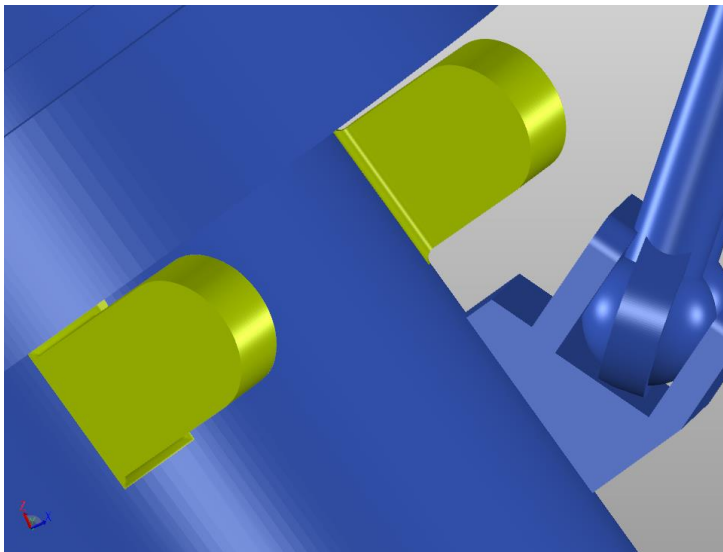

Figure 5. Multi-scale geometry features
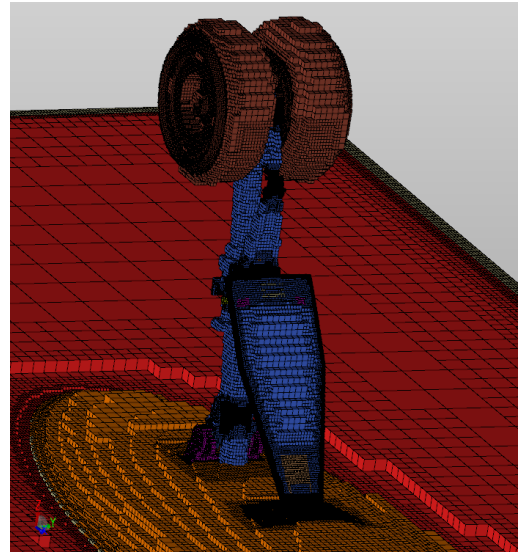
Figure 6. Octree mesh cells

American Institute of Aeronautics and Astronautics
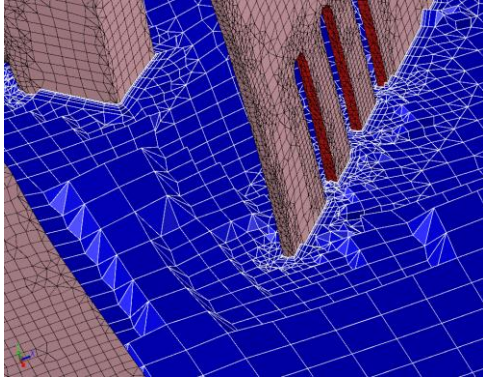
Figure 7. Boundary layer mesh
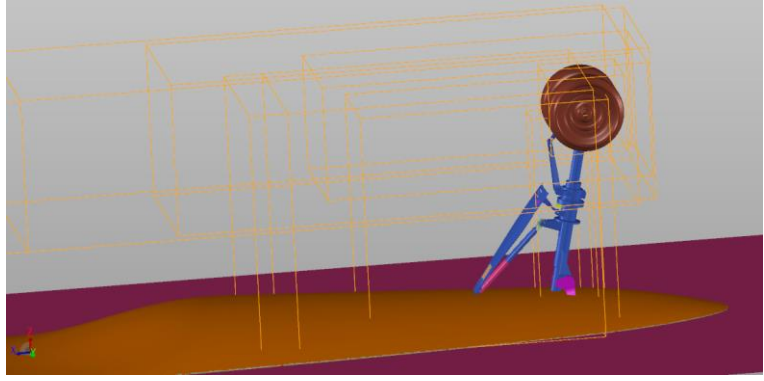
Figure 8. Volume mesh refinement
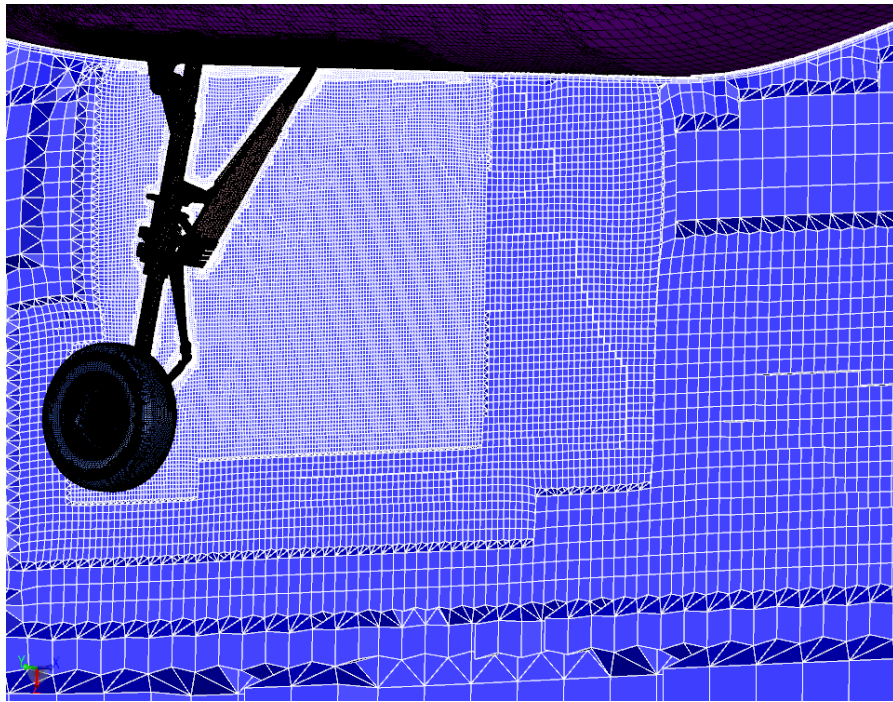
Figure 9. Isosurface of 3D volume mesh to show volume refinement

The complexity of the landing gear is presented in Fig.3 - with all real geometry parts and connections preserved and resolved. Hence, to generate an appropriate mesh to support the high geometry fidelity simulations is a key challenge for the current simulations. The first difficulty is to deal with dirty CAD with errors such as unsealed gaps as shown in Fig. 4. Another difficulty is the multiple scales of the geometry as clear in Fig. 5 with many small geometry features. An implicit geometry model using Level Set distance fields was adopted to handle multiple-scale complex geometries in our BOXERMesh - the near wall front octree mesh is presented in Fig. 6 and an isosurface of the volume mesh indicating boundary layer cells is shown in Fig.7. In order to capture the acoustic field more accurately, volume refinement was applied mainly around the downstream of the landing gear as shown in Fig.8 and the resulting mesh is presented in Fig.9. High order meshes are necessary to support the high order simultions, and the cell count must be very strictly controlled because the degree of freedom efficiency is much higher than for traditional for FVM and FDM approaches but has rather higher per cell computing cost requirements. Hence, high order coarse meshes are necessary to manage and optimise the overall computing cost. Examples of the high order surface mesh for the landing gear for current simulations are presented in Fig. 10, Fig. 11 and Fig.12 – all which are rendred by GMSH[12].
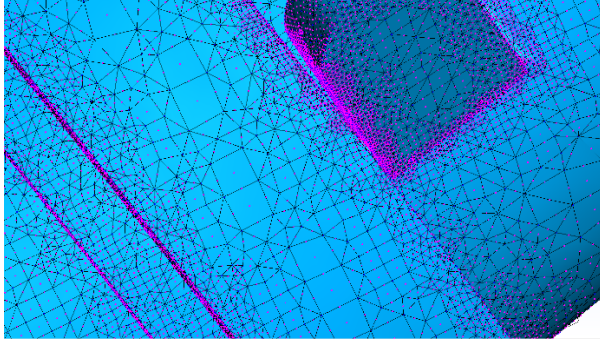
Figure 10. High order mesh around strut
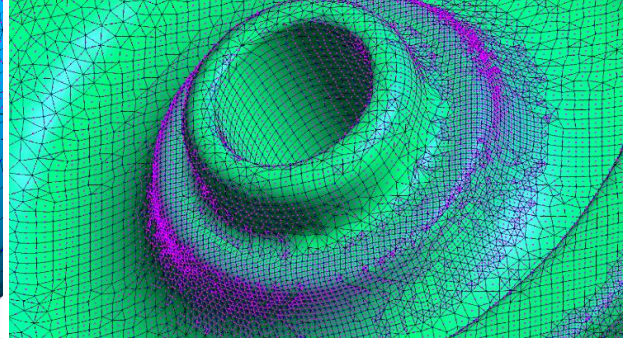
Figure 11. High order mesh around the tyre
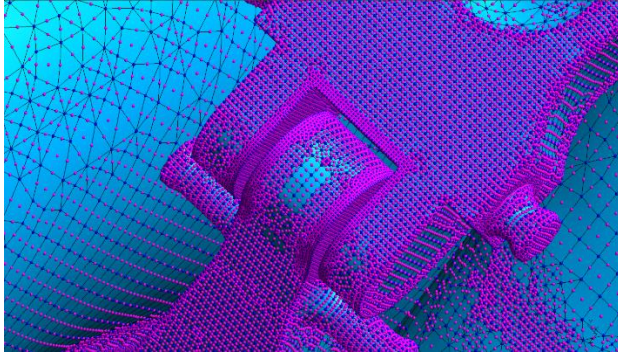

Figure 12. High order mesh around the door
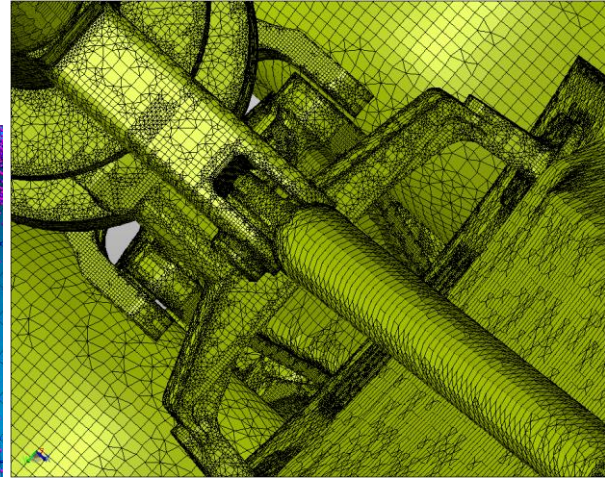
Figure 13. Surface mesh for complex geometry

III. Governing Equations and Flow Solver Configuration

The flow solver code based on high order STEFR method, HOTNewt, under development at Cambridge Flow Solutions Ltd, uses general unstructured meshes to solve wide range of problems[5,8,9,11]. In this case, implicit LES without any explicit sub-scale model is performed to solve the Navier-|Stokes equations and an adaptive non-equilibrium wall-model is adopted to deal with near wall regions where the flowfield in the sublayer can't be fully resolved with adequate mesh density. As shown in Fig.7~Fig.12, second order meshes were generated and smoothed, with information given in Table 1.

Table 1. Statistic of mesh and solver information

Number of cells	Order of accuracy	Number of DOFs	Memory comsumpti-on (GB)	Maximum(~) local time step(s), dt_{max}	Minimum(~) local time step(s), dt_{min}	Coarsest cell size (mm)	Finest cell size (mm)
11175544	THIRD	862615440	301.1	$3.34e-05$	$6.12e-10$	114.3	0.0018

In the STEFR method, accurate unsteady simulations like LES are achieved with local timestepping for each cell, as shown in Fig. 14. In the present application the ratio of the maximum timestep and minimum timestep (dt_{max}/dt_{min}) is 54575.163, which means the saving in computing cost is huge. In the actual implementation of the STEFR method, the ratio between local time step of each single element and the global mimumum timestep (dt_{min}) is set as a power of 2 ($dt = dt_{min} * 2^{level}$), and the statistics for all levels for the whole mesh is presented in Table 2.

Table 2. Statistic for time levels

Level id	Dimentional timestep (dt_{min})	Number of cells for each level	Number of cells percentage	Computing cost weight percentage
Speed up ratio associated with local time-stepping: **34.8458**. Number of levels: 16				
0	1	338	0.0030245%	0.102519%
1	2	9638	0.0862419%	1.587391%
2	4	304132	2.7214067%	26.60469%
3	8	617759	5.5277757%	25.8613%
4	16	613929	5.4935044%	12.265%
5	32	2143459	19.179907%	16.2188%
6	64	2841337	25.424597%	11.3162%
7	128	1637243	14.650231%	3.8044%
8	256	873911	7.819852%	1.138%
9	512	813052	7.2752789%	0.5344%
10	1024	942977	8.4378622%	0.499%
11	2048	238835	2.1371219%	0.0565%
12	4096	85562	0.7656182%	0.0095%
13	8192	34416	0.3079582%	0.0019%
14	16384	10017	0.0896332%	0.0002%
15	32768	8939	0.0799872%	0.0002%

It can be seen that level 2 only has about 314k elements(about 2.72% of total elements), but the computing cost is over 26%. In contrast, level 7 takes more than 14.65% of the total elements but only costs 3.8% of the total computing resource - and level 10 takes about 8.43% of the total element but even then only costs 0.499% of the total computing resource. The speed up ratio is about 34.8458 compared to the use of classical, uniform time stepping for the current simulations.

IV. Implementation on heterogeneous computing system including many-core processors

Many-core computing systems are widely used and have progressed rapidly in recent years because of its high cost- effectiveness compared to pure, "traditional" multi-core CPU computing system in the HPC area. These computing systems are based on different many-core units including NVIDIA Tesla GPUs, AMD GPUs and Intel PHI co-processors. As is clear from the numerical review of the STEFR method earlier, its time marching method is not uniform and the data-communication is irregular. Also, for some computing loops of a single time marching step, the number of executive elements is maybe quite small especially in the final stage of inner iterative as shown in Figure 14(e)~ Figure 14(g). Therefore, several available many-core units have physical computing threads which are not suitable for STEFR method, such as NVIDIA Tesla GPUs and AMD GPUs. As reported in this paper, the Intel PHI co-processors have been chosen to build our heterogeneous computing system in order to trade fewer computing cores against each physical core having much stronger computing ability.

To support this work we built a heterogeneous many-core computing system consisting of 8 nodes, each node has 2 Intel Xeon CPUs each with 8 physical cores and 6 many-core Intel PHI cards each with in turn 57 physical cores. All components are commodity items, easily and cheaply available. The system architecture is illustrated in Figure 15. This type of system holds out great promise going forward for a step change reduction in hardware costs – and hence, if the system can be driven efficiently, a step change reduction in LES solution time scales and cost.

There are three different types of data-communication used in the computing system as shown in Figure 3: CPUs to CPUs, PHI co-processors and CPUs, internal data-communications between PHI co-processors/CPUs. Due to the irregular time marching process, the principle behind the design of the data-communication model is to reduce the usage of distributed memory, and make use of more communication latency. As shown in Figure 16, asynchronous MPI is used for communication between CPUs though Infiniband (which has already demonstrated its high efficiency [5][8]).The data-transfer performance for small packages of data between host CPUs and PHI cards using Intel MPI is very poor even using OFED, therefore the "offload mode" [13] code was written which has

mirror memory on host CPUs of all data-structures allocated on PHI co-processors and which speeds up the data transfer process. For each of the many-cores on host CPUs of each node, and on each PHI coprocessor, all executive loops are performed on shared-memory by using OpenMP's multi-threading method. In order to reduce small package data-communication, the "offload mode" data transfer is synchronous between CPUs and PHI coprocessors, there is no communication between different PHI coprocessors and between PHI co-processors and CPUs on other nodes by using smart partitioning.

Another challenge for modern many-core computing units is the limited memory (8GB per PHI coprocessor) compared to CPUs (128GB per node). From the numerical scheme review in Section 1.2, in the STEFR method, the computational cost for single cell depends on its smallest size (and associated time limit) - however, the memory consumption still scales with the element number. So, in this work, a special multi-level, multi-constraint smart partitioning algorithm was written, to automatically allocate more small size elements to PHI co-processors (typically near wall boundary layer elements) and put more elements on the CPUs to maintain load balancing and reduce data-communication size.

All above effort allows and enables the small cluster to perform large scale high order Large Eddy Simulations for the landing gear case with about 0.8 billion DOFs.


(a). $i_{iter} = 1$ (b). $i_{iter} = 1$ (c). $i_{iter} = 1$ (d). $i_{iter} = 1$

(e). $i_{iter} = 41$ (f). $i_{iter} = 51$ (g). $i_{iter} = 61$ (d). $i_{iter} = 176$
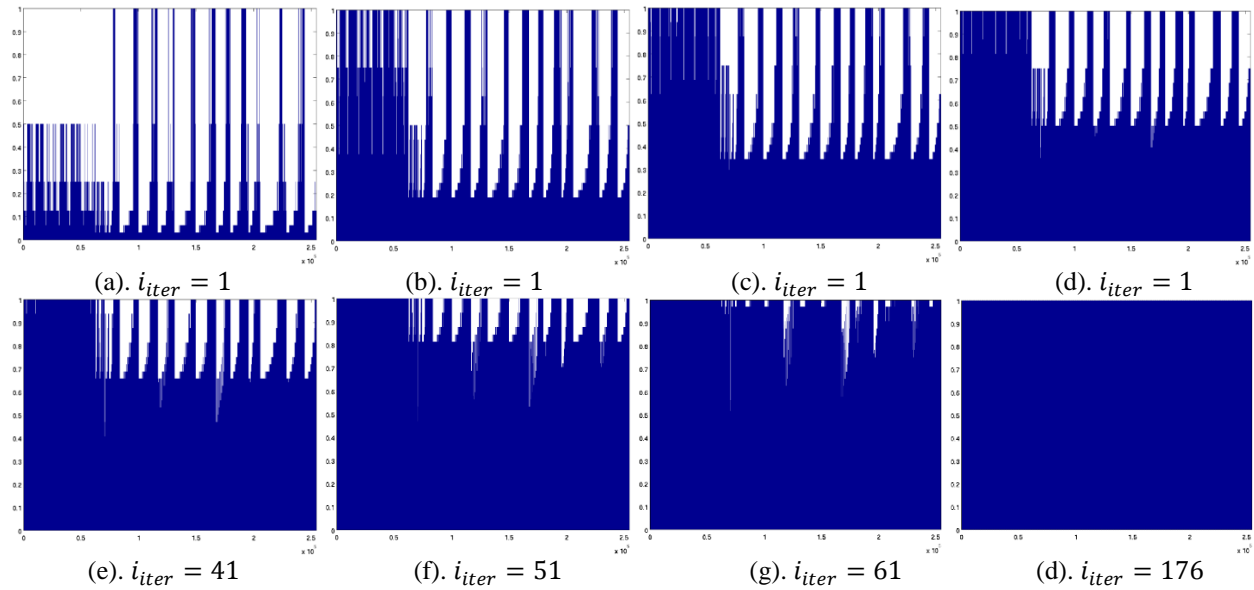
Figure 14. Snapshots for time marching of one step:
**horizontal is element index and vertical is normalized prediction time.**
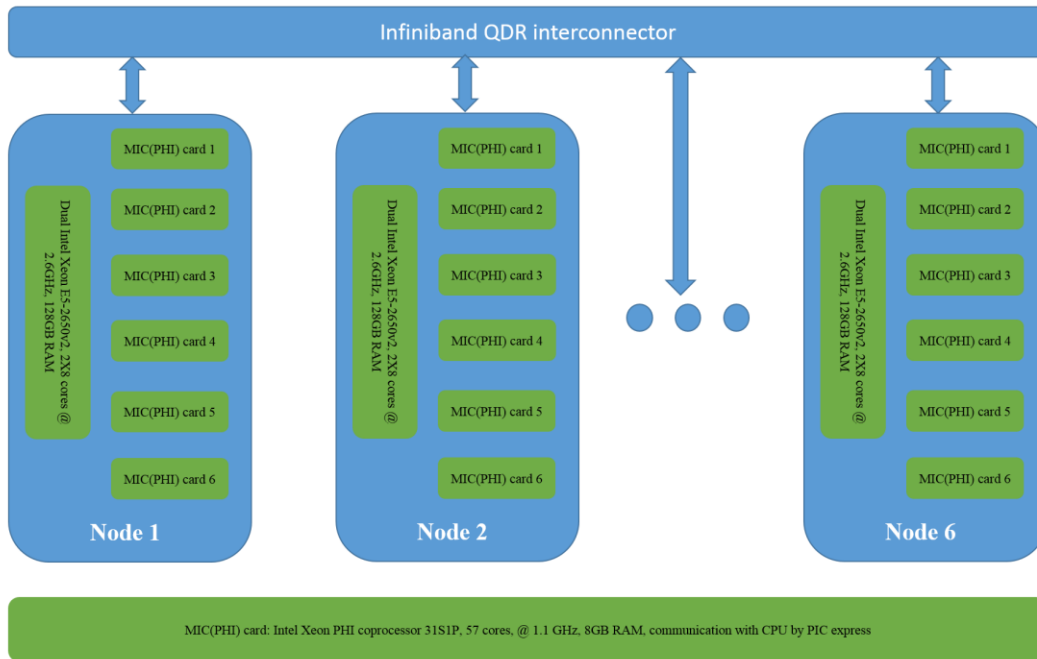
Figure 15. Heterogeneous computing cluster
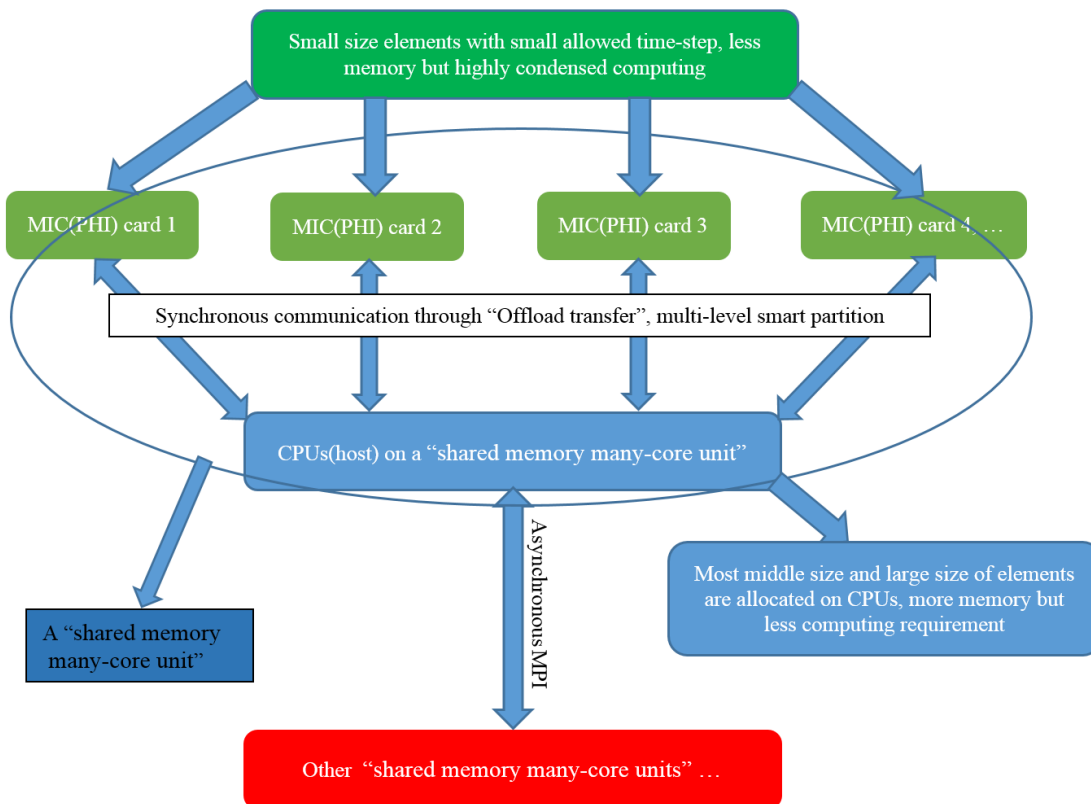
**Figure 16. Communications between different computing units including CPUs and MIC cards.**
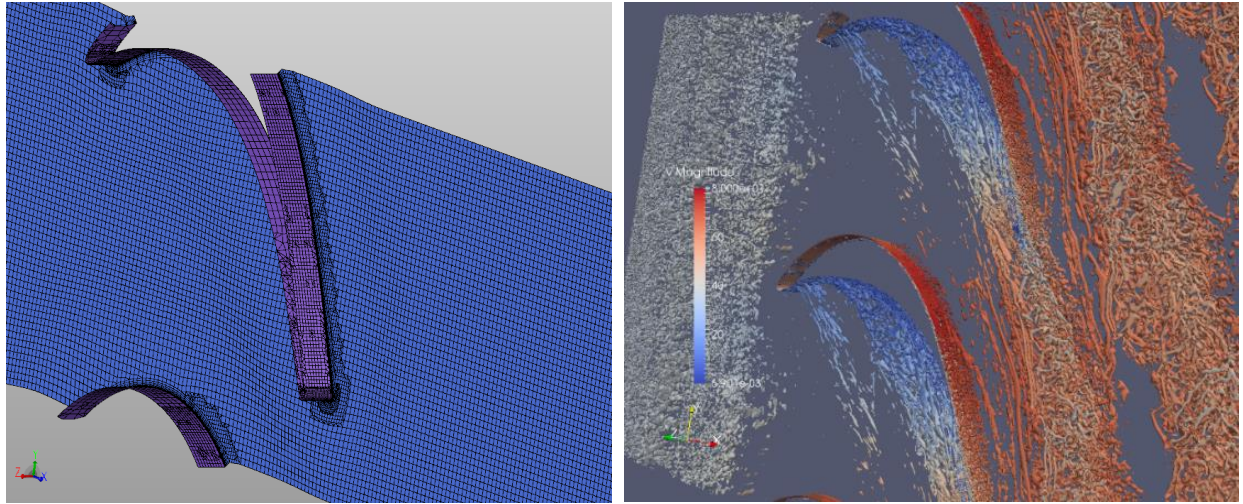
(a) **Mesh for test case T106A**

(b) **. ISO-Surface of Q-criterion for transient result**
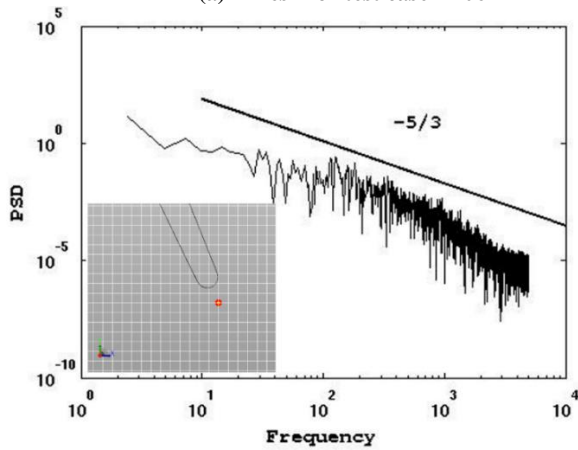
(c) **PSD of total velocity within the blade wake** (d) **RMS velocity profiles around the transitional zone**
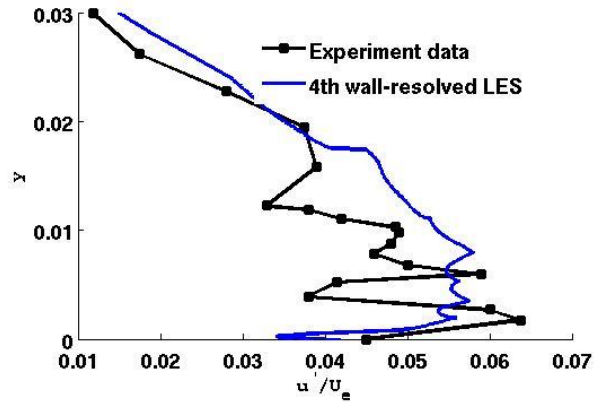
Figure 17. RMS velocity profiles around the transitional/separation zone; measurements and predictions using data from Case T106A-4 (110K hybrid unstructured code, 4th order accurate, and wall-resolved with near wall Y$^+$ ~ 5) [14], running on only one node of the small heterogeneous computing system

As an introduction to the potential of the present LES method and its novel computing hardware implementation Figure 17 presents some results for a high lift low pressure turbine blade [14], which only used one node of the computer but it able to deliver wall-resolved high order LES/DNS results very fast and agree with experimental data very well.

V. Results and Analysis

This main results section will describe and discuss the application of the present LES method to the landing gear configuration. The initial flow field (velocity magnititude) from a basic steady first order implicit iterative solver is shown in Fig. 18 – this is used to initialize and launch the LES.
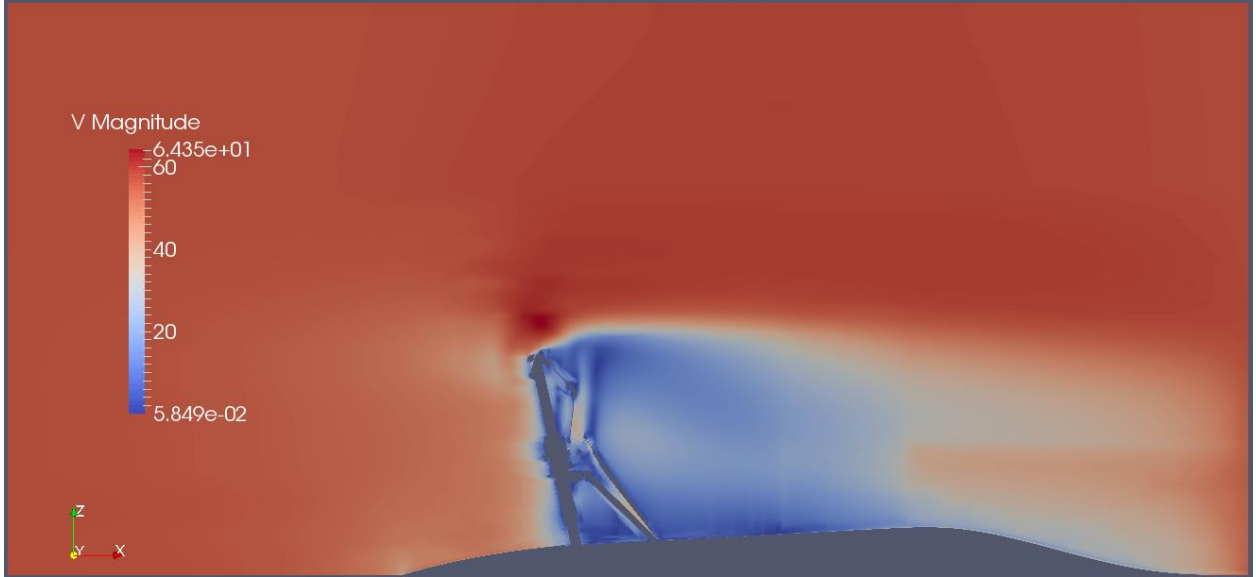

Figure 18. Initial flow field from steady first order implicit interative solver.

Then second order and third order simulations were performed on 1 node and 8 nodes respectively of the computer cluster and the simulation statistics are listed on Table 3 - where 1 T_p represent the physical time for flow passing the strut of the landing gear. The wall-clock times are remarkably small for a simulation of this size and on computer hardware of this low cost.

Table 3. Simulation statistics

Case ID	Near wall resolution	Order of accuracy	Speed Up Ratio	Number of nodes on cluster	Memory comsuming(GB)	Wall-clock time for $1T_p$(hours)
Landing-Gear-1	Partly Wall-resolved	2nd	34.4	1	90.6	10.2
Landing-Gear-2	Partly Wall-resolved	3rd	34.85	8	292	18.7

Figure 19 present Q-criterion for transient results of 2nd and 3rd simulations respectively, it could be found the basic structures are quite similar but 3rd simulation resolves more detail flow structures. Figure 20 present the transient magnititude of velocity on different slice positions and which indicate the third order simulation captures very good detail transient flow structures. Flow structures on different regions along surface the landing gear geometry are shown in Fig.21. In order to compare with aerodynamic experiment data, the solution were extracted on PIV measurement plane as shown in Figure 25. The spanwise vorticity of 2nd order simulation and 3rd order simulation are presented and compared to experiment data. The comparison of surface pressure along the middle plane on port wheel(plane 3 on Figure.25), is given in Figure 27, it could be found the higher order simulation agree much better than 2nd order simulation, and no obvious uner-estimation between $\theta = 100{\sim}170$ which happens on other simulations based on 2nd finite volume method[2].
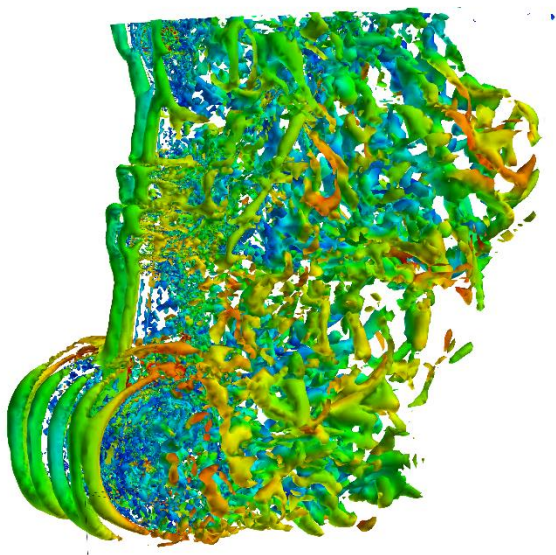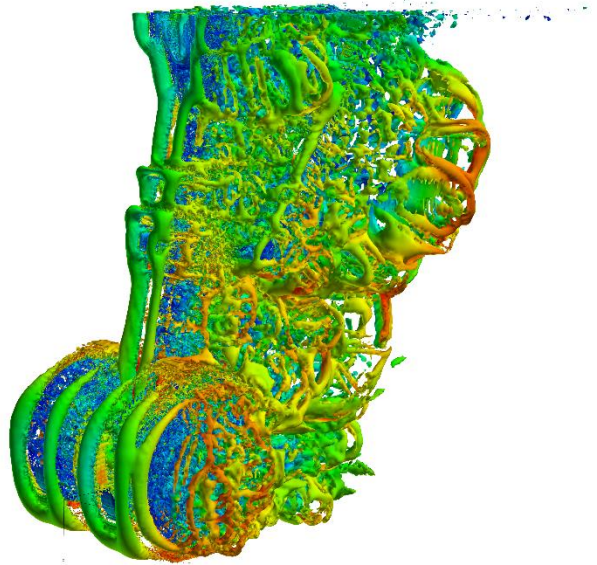
(a)2nd order simulation   (b)3nd order simulation
Figure 19. Q-criterion for transient result of 2nd and 3rd simulations, Q=3 $\times$ 10^{5}
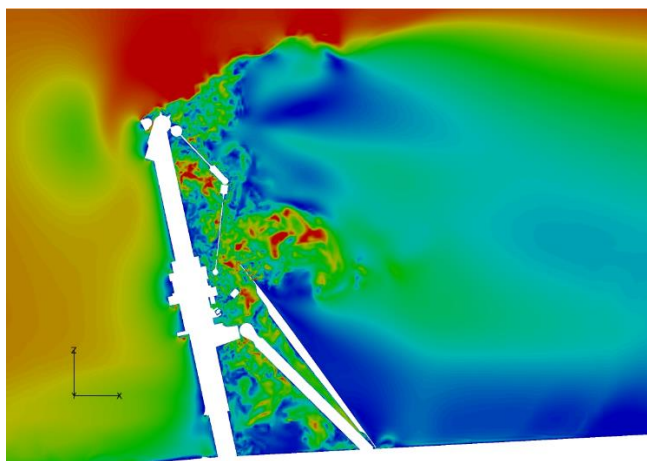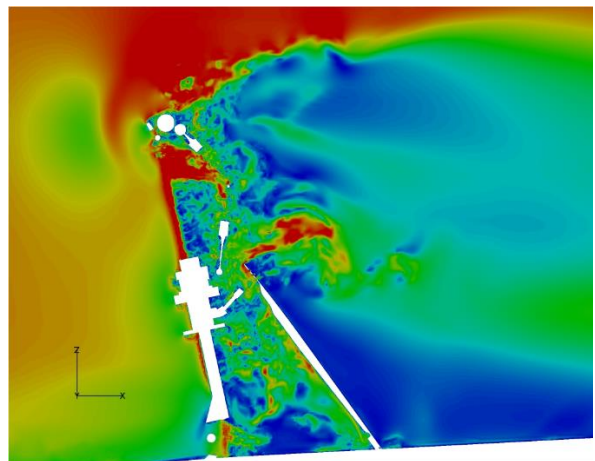

(a)Y=0   **(b) Y=0.01**
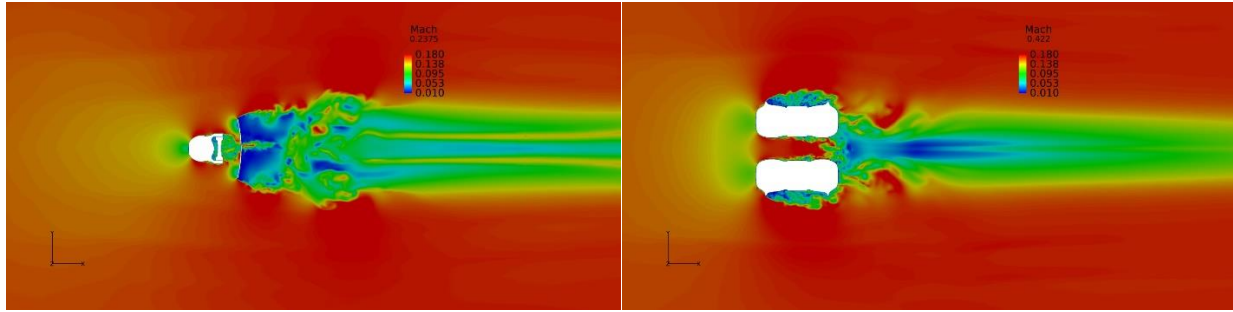
(c)z=0.2375

(d)z=0.422
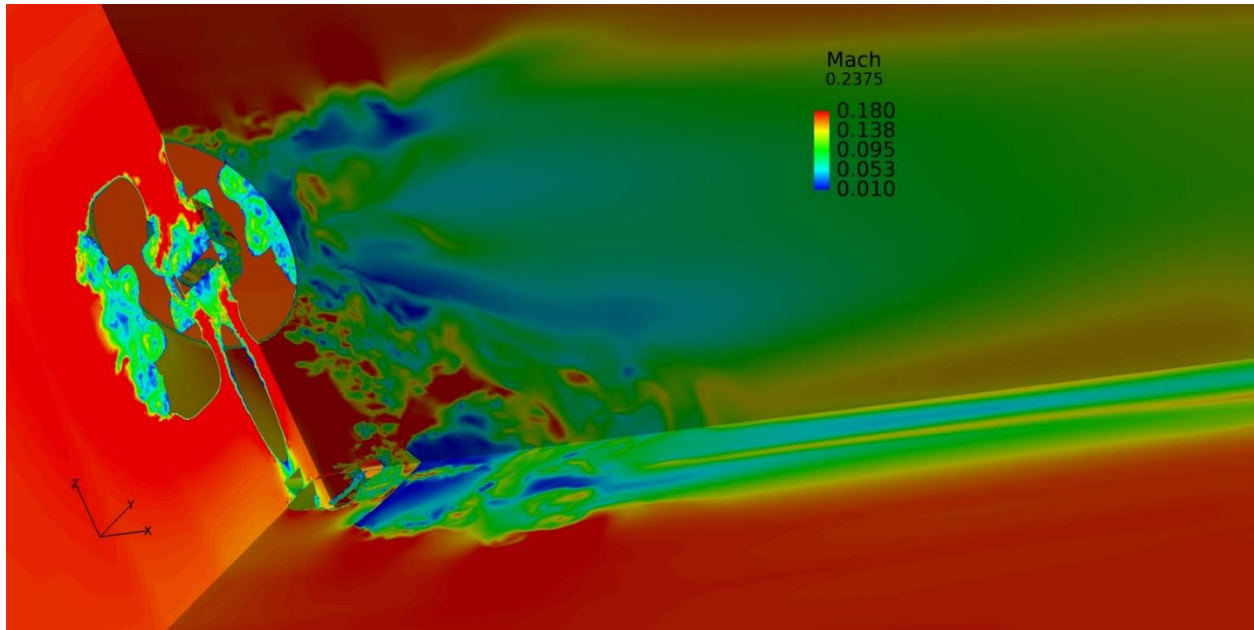
(e) x=0.26, y=0.02, z=0.2375

Figure 20. Transient Mach number on different slices of the landing gear flow filed, 3rd simulation
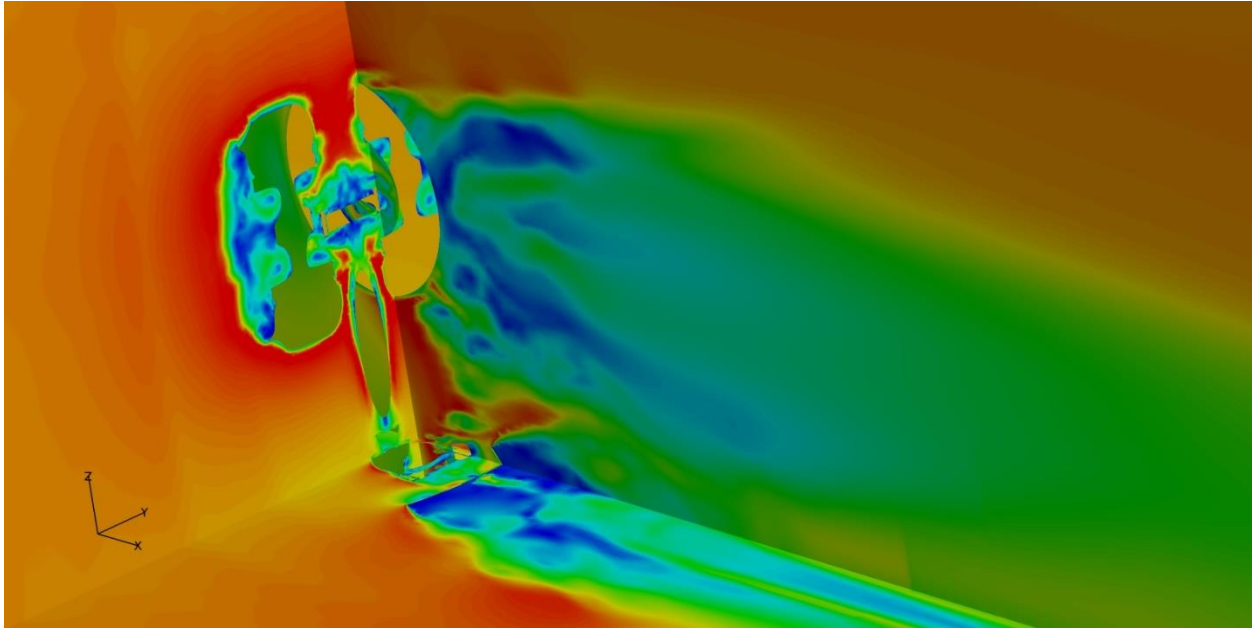
**Figure 21. Mean Mach number on different slices of the landing gear flow filed, 2ⁿᵈ simulation**
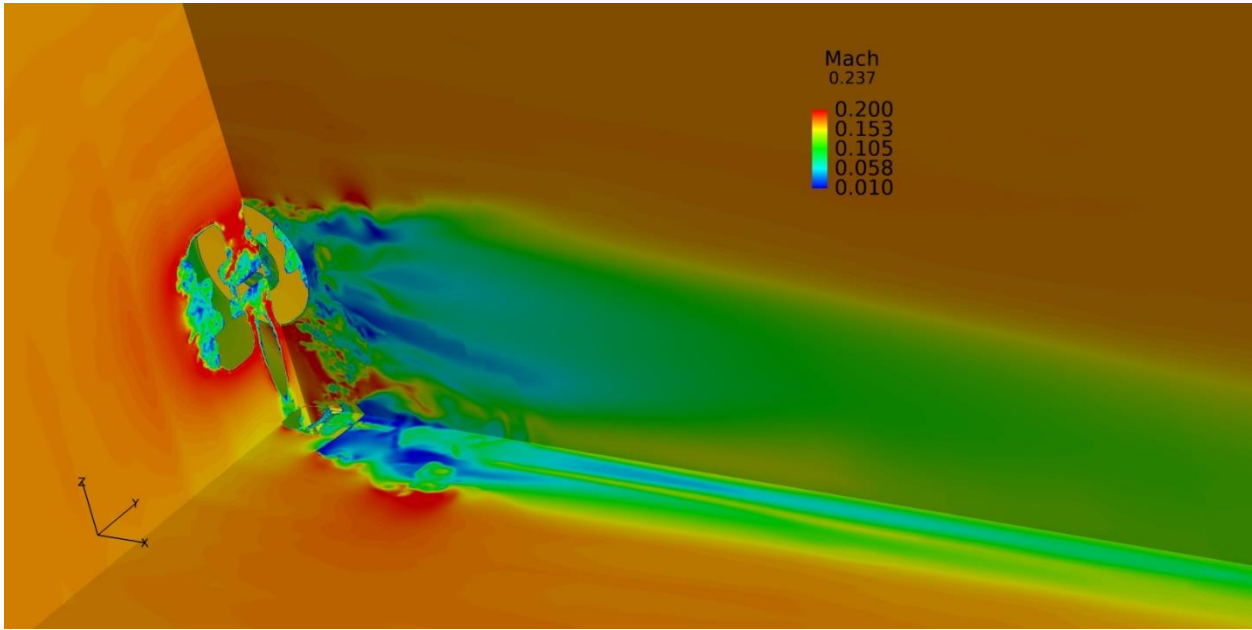

Figure 22. Mean Mach number on different slices of the landing gear flow filed, 3ʳᵈ simulation
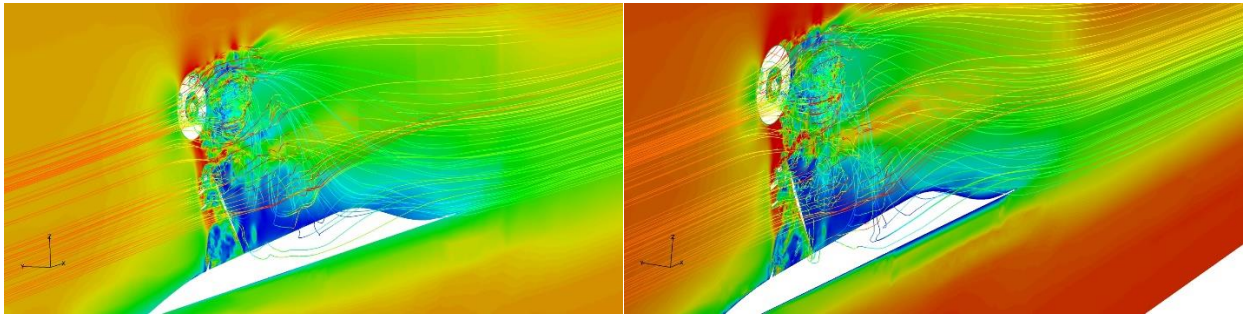
(a)2nd simulation   (b)3rd simulation

Figure 23. Transient streamlines around the landing gear colored by Mach number, with slice y=0.02
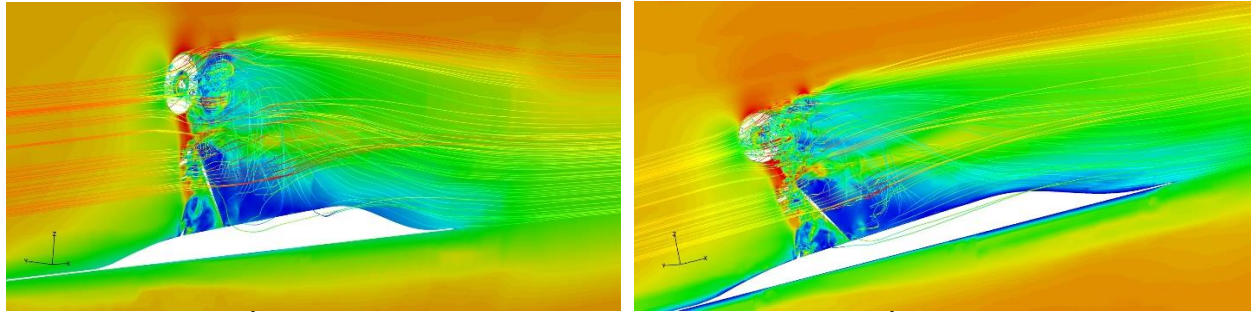
(a)2nd simulation   (b)3rd simulation

Figure 24. Mean streamlines around the landing gear colored by Mach number, with slice y=0.02
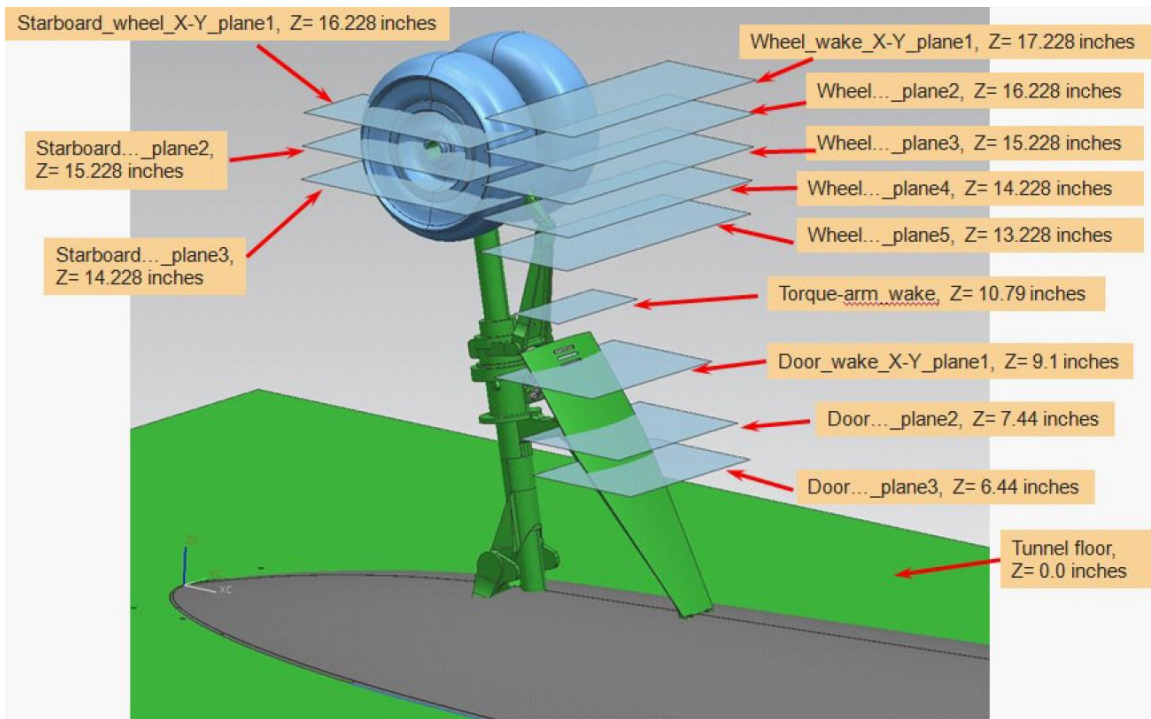
**Figure 25. PIV measurement planes for BART experiment set up[2].**
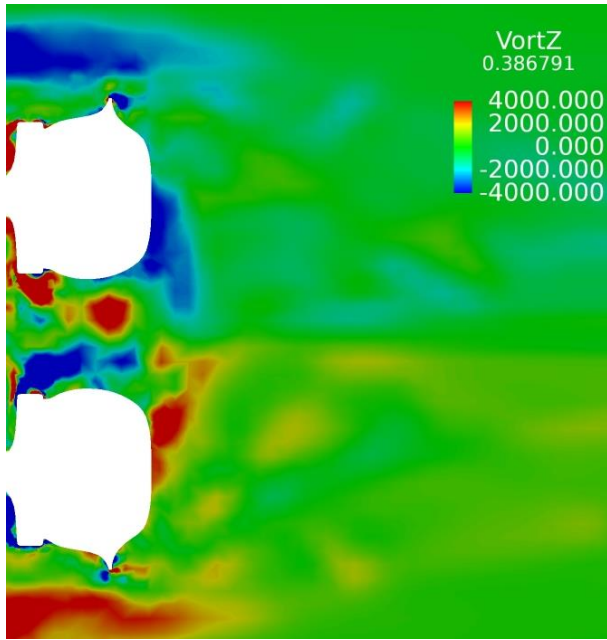
(a)2nd simulation
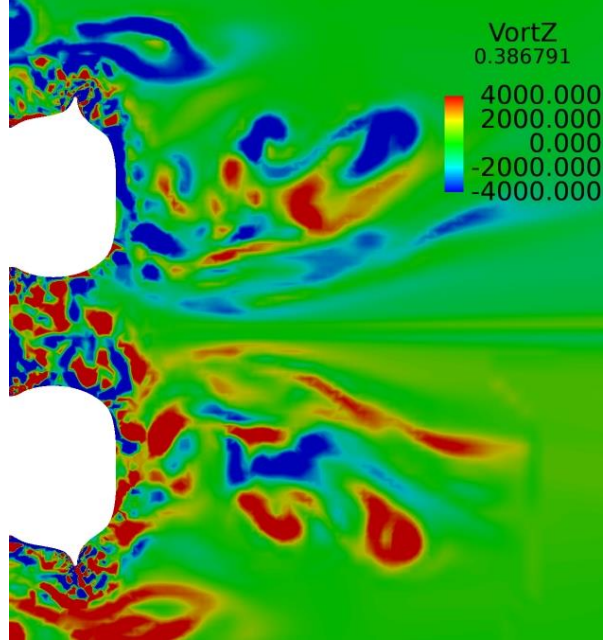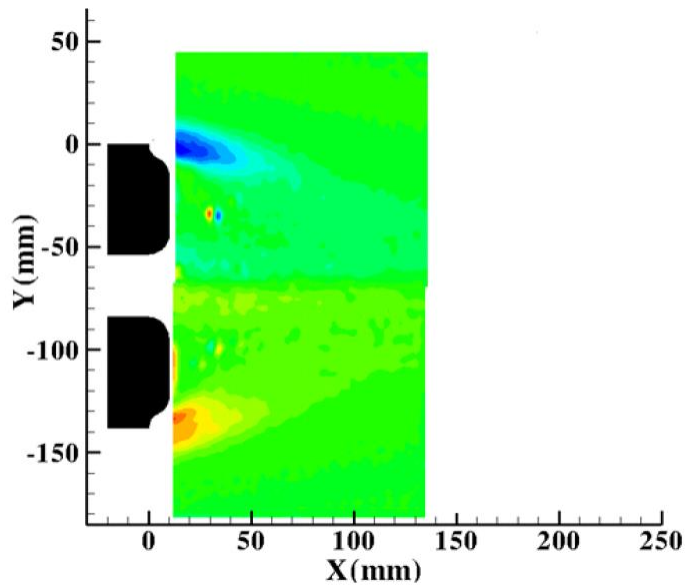
(b) 3rd simulation

(b) Experiment PIV data

Figure 26. Spanwise vorticity contours, mid-wheel plane(plan 3 shown in Fig.25).
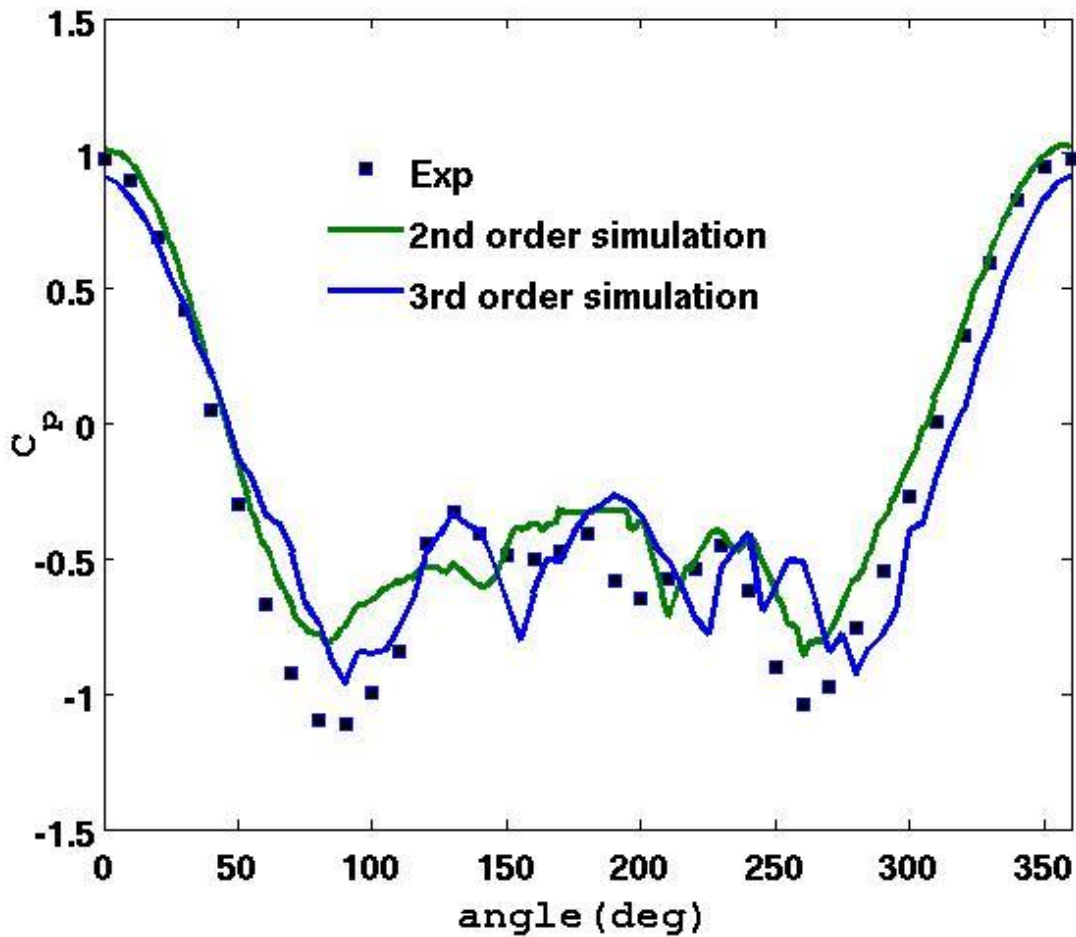
Figure 27. Surface pressure distribution on port wheel.

VI. Concluding Remarks

High order wall-modelled Large Eddy Simulations for the complex flowfield of the real geometry landing gear were performed on a heterogeneous computing system consisting of traditional cpu processors and Intel PHI many-core co-processors.

These large scale simulations for multiple scale, complex geoemtries were demonstrated to be able to be performed on limited computing resource with low running cost. This was achieved by innovative contributions in both mesh generation, numerical algorithm design and efficient hardware implementations. The wall-clock times are remarkably small for a simulation of this size and on computer hardware of this low cost.

Future work will focus on post-processing which is now clearly the key bottleneck.

Acknowledgments

References

[1]M. R. Khorrami, D. P. Lockard, Jr. W. M. Humphreys, M. M. Choudhari and T. Van de Ven, "Preliminary Analysis of Acoustic Measurements from the NASA-Gulfstream Airframe Noise Flight Test," AIAA Paper 2008-2814, May 2008

[2]V. N. Vatsa, D. P. Lockard and M. R. Khorrami, "Application of FUN3D Solver for Aeroacoustics Simulation of a Nose Landing Gear Configuration", AIAA Paper 2011-2820, June 2011

[3]V. N. Vatsa, M. R. Khorrami, M. A. Park and D. P. Lockard, "Aeroacroustic Simulation of Nose Landing Gear on Adaptive Unstructured Grids with FUN3D", AIAA Paper 2013-2071, May 2013

[4]http://www.cambridgeflowsolutions.com

[5]Y. Lu, K. Liu, and W. N. Dawes. "Flow simulation system based on high order space-time extension of flux reconstruction method". In AIAA Science and Technology Forum and Exposition(SciTech2015), AIAA2015-0833, Jan 2015.

[6] Huynh, H. T. "A flux reconstruction approach to high-order schemes including discontinuous Galerkin methods", 18th AIAA Computational Fluid Dynamics Conference, 2007, AIAA 2007-4079

[7]Y.Lu. "Local Reconstruction High Order Method and Experimental Research for Internal Flow of Turbomachinery". *phD thesis*, Tsinghua University, China.

[8]Y. Lu, K. Liu, and W. N. Dawes. "Large eddy simulations using high order flux reconstruction method on hybrid un-structuredmeshes". In AIAA Science and Technology Forum and Exposition(SciTech2014), AIAA2014-0424, Jan 2014.

[9]Y.Lu, W.N.Dawes, "High order Large Eddy Simulations for a transonic turbine blade using hybrid unstructured meshes", ASME Paper, GT2015-42283.

[10]N. Zawodny, F. Liu, T. Yardibi, L. Cattafesta, M. Khorrami, D. Neuhart and T. Van de Ven, "A Comparative Study of a ¼-scale Gulfstream G550 Aircraft Nose Gear Model", AIAA Paper 2009-3153. May 2009

[11]Y. Lu and W.N.Dawes, "High order large eddy simulations for a transonic turbine blade using hybrid unstructured meshes", AMSE Paper GT2015-42283, June 2015

[12]http://geuz.org/gmsh/

[13]Jim Jeffers and James Reinders. Intel Xeon Phi Coprocessor High-Performance Programming, 2013

[14]Y. Lu, K. Liu, and W. N. Dawes. Fast high order large eddy simulations on many core Computing systems for turbomachinery, ASME-Paper, GT2016-57468, submitted

American Institute of Aeronautics and Astronautics